Two dimensional anomalous small-angle scattering measurements at the Mg K absorption edge for nanostructure analysis in concentrated Al-Mg alloys

AUTHOR(S):

Okuda, Hiroshi; Sakohata, Rei; Lin, Shan; Kitajima, Yoshinori; Tamenori, Yusuke

Template for APEX (Jan. 2014)

Two dimensional anomalous small-angle scattering measurements at the Mg K absorption edge for nanostructure analysis in concentrated Al-Mg alloys

Hiroshi Okuda[1]*, Rei Sakohata [1],Shan Lin[1], Yoshinori Kitajima[2], Yusuke Tamenori[3]

[1]*Department of Materials Science and Engineering, Kyoto University, Kyoto 606-8501, Japan*

[2]*Photon Factory, High Energy Accelerator Research Institute,Ibaraki 305-0801, Japan*

[3]*Japan Synchrotron Radiation Research Institute, Hyogo 679−5198 Japan.*

E-mail: okuda.hiroshi.5a@kyoto-u.ac.jp

Two dimensional anomalous small-angle scattering measurement at K absorption edge of Mg has been successfully demonstrated for concentrated Al-Mg binary alloys and MgO nanoparticles. Enhancement of contrast between Mg-rich precipitates and Al matrix was explained by anomalous dispersion of Mg, and anisotropic SAXS pattern agreed with the microstructure observed by TEM. Agreement of atomic scattering factor obtained from Al-Mg and MgO nanoparticles indicates that the origin of SAXS in the present Al-Mg alloys is Guinier-Preston zones, not the voids that grew from supersaturated vacancies.

Controlling nanostructures undergoing phase transformation or self-organization processes is important to optimize their properties, not only for structural materials but also for functional materials. For light metal materials, Al- and Mg-based alloys with relatively small addition of solute elements have been developed for energy-efficient structural materials for transportation [1-3]. To add with such traditional use, for example, potential use for battery materials require microstructural assessment of much concentrated alloys. However, weak contrast between Al and Mg, and lattice strain due to difference in the atomic size made characterization of the microstructure of such concentrated Al-Mg alloys difficult by conventional transmission electron microscopy (TEM) or hard X-rays, in particular, in the early stage of phase transformation. Small-angle X-ray scattering (SAXS) has been used to obtain quantitative information on the nanostructures as an averaged quantity over macroscopic volume, ranging from hard metallic materials to soft materials [4-6]. Particularly the method is useful to obtain average nanostructural information for materials that are poorly ordered and have larger volume fraction, such as spinodally decomposed nanostructures and porous materials. However, the elements that we are interested in the present work, Mg and Al are neighboring elements, and the contrast between the Al matrix and Mg-rich precipitates is even weaker because the precipitates, i.e., the composition of GP zones or β'' is assumed to be less than a quarter, Al_3Mg [7-11] for $L1_2$ ordered structure. Further, Al-Mg alloy often contains large amount of vacancies and hydrogen depending on the process history[12-14]. Therefore, we need a method to identify the origin of the contrast. Such conditions are often encountered in examining advanced materials, for example, sulfur in Nafion® film[15], phosphorous in membranes[16,17]. Anomalous small-angle X-ray scattering (ASAXS) enhances otherwise weak scattering contrast by choosing the photon energy close to the absorption edge of the element interest[18-20], and is also useful to discuss the origin of the contrast by examining the energy dependence of the contrast[19,21]. In the present work, we demonstrate ASAXS results at lower side of the so-called tender X-rays region, where prevailing pixel detectors like Pilatus extended down to Si K edge[22,23], is still not available, for anisotropic samples.

Samples used in the present work are Al-15.8 mass% Mg. Alloy ingot have been cut into a block of about 0.6 cm x 0.6 cm x 4cm and homogenized at 723 K for a week in vacuum. The grain size of the present samples, ranging between 0.3 mm and 3 mm as observed by an

optical microscope was larger than the beam size used in the present SAXS measurements. The block was then sliced into plate with 1mm thickness, and solution treated at 723 K for 300 s, quenched into iced water, and aged at 313 K in an oil bath. Differential scanning calorimetry (DSC) measurements have been made at a heating rate of 10 K/min. to compare precipitation microstructure with previous works[7,8,24]. Good agreement on the dissolution temperature and heat of dissolution of GP zones was obtained. The sample was thinned down to about 20 micrometers to obtain reasonable transmission for the transmission SAXS measurements. The measurements were performed at beam line 11A of Photon Factory, KEK and beamline 27SU of SPring-8, Japan. Details of the beamlines are described in ref.25. Two-dimensional SAXS intensity was measured by P45 phosphor coupled with tapered optics (FOT) and a CCD detector cooled down to 233 K. Detail of the measurement system is given in [26], where the measurements have been made at the K absorption edge of Al for the samples that have strong scattering contrast with isotropic profile. Calibration of scattering angle was made by the Debye rings of silver behenate[26,27], where isotropic rings with uniform intensity along the rings were observed, showing that distortion correction is not necessary.

Figure 1 gives the change of specific heat of Al-15.8%Mg samples aged at 313 K. Although several metastable phases are reported for Al-Mg binary alloys[28,29], only one isolated dissolution peak was observed, which was attributed to GP zones. The area of endothermic peak identified as GP zones increased in the early stage of aging, and then the enthalpy saturate to a value that agreed with reported ones s[7-9,24]. Therefore, the present sample contains GP zones whose volume fraction agree with the preceding works. The specific heat in Fig.1 shows an apparent two peaks. However, this does not necessarily means two different phases as suggested by several works[7,8], but is rather related to kinetic effect of dissolution[30].

SAXS intensity from particle systems can be described as[4,5,31,32] ;

$$I(q) = I_0 N < v >^2 \Delta\rho^2 |\Phi(qR)|^2 S(q) \qquad (1)$$

where I_0, N, v, $\Delta\rho$, $\Phi(qR)$, S(q) are a proportional constant, number density of the precipitates, volume of precipitates, scattering contrast between the matrix and the precipitates, the form factor and the structure factor of the precipitates, respectively. q and R are the magnitude of scattering vector and the radius of the precipitate.

Figure 2 shows two dimensional ASAXS profiles for Al-Mg samples aged for (a)1day, (b) 3days and (c) 2weeks. The measurements were made at E=1.298 keV, where the contrast is enhanced by anomalous dispersion. The scattering profile is isotropic in the early stage of aging for 1 day as shown in Fig.2(a), and the anisotropy of scattering intensity develops with increasing aging time. As reported by TEM observation, phase separation induces an anisotropic image whose direction of modulation lies along <100>[8,24] after longer annealing time. The scattering patterns in Fig. 2(b) and (c) clearly show 4-fold anisotropy. Equation (1) suggests that the origin of the anisotropic scattering in Fig.2(b) and (c) is either the anisotropy in the shape of GP zones, $\Phi(qR)$, or that in the spatial arrangement of GP zones, $S(q)$ [5,30,31]. The gyration radius, R_g, for <100> directions and <110> directions agreed for Fig. 2(a)-(c), with R_g=1.9, 2.6 and 4.0 nm respectively. In contrast, the interparticle distance was 3% longer in <110> direction for Fig.2(b) and 5% longer for Fig.2(c), where the average interparticle distance was 9.0 nm 9.9 nm, and 14.5 nm for Fig. 2(a)-(c) respectively. This suggests that anisotropic microstructure appearing in the later stage of phase separation in the present alloy is characterized by anisotropic arrangement of GP zones, while the shape of GP zones remains isotropic. From eq. (1), ASAXS intensity simply changes in proportional to the square of the scattering contrast, $\Delta\rho^2(E)$ for the binary case. Figure 3 (a) gives the change of radially averaged SAXS intensity obtained for an Al-Mg sample aged for 3 days. The contrast, $\Delta\rho$ is expressed as

$$\Delta\rho = (f_{Al}/v_{Al} - f_{Mg}/v_{Mg})(c_p - c_m), \qquad (2)$$

where c_p and c_m are the Mg concentration of the GP zones and the matrix, and v_{Al}, v_{Mg} are the atomic volume of each element. The scattering intensity increased as the incident photon energy increased to reach the absorption edge, in agreement with the change in $\Delta\rho$. In contrast, if the origin of the SAXS is nanovoids as often reported for AlMg alloys under some process conditions, such as cast under humidity or under plastic strain[12-14] which is very important for mechanical properties such as fatigue and fracture of the materials, the contrast between the Al matrix and voids behaves oppositely, i.e., the contrast decreases as the photon energy increases. Therefore, although the scattering contrast is much stronger for the voids, present results confirm the analysis model based on phase separation structure. Figure 3(b) gives the ASAXS profiles for MgO nanoparticles. This case, origin of the scattering contrast is that between MgO and vacuum : $\Delta\rho = (f_{Mg} + f_O)/v_{MgO}$. The

ASAXS intensity decreases in parallel as the photon energy increases as expected by eq.(1). The Porod's law[31,32] with the power law of q^{-4} was observed. To examine anomalous effect on the ASAXS intensity, the real part of atomic scattering factor of Mg, $f_{1(Mg)}$, was calculated from ASAXS intensity. For magnesia nanoparticles, taking the atomic scattering factor at the energy far enough from the absorption edge, E=1.266 keV, given by Cromer-Libermann[33,34] as standard, the scattering factor of Mg at energy E is calculated from the relative change of SAXS intensity, I(q,E)/I(q, 1.266 keV) by

$$f^{E}_{1(Mg)} = \sqrt{I(q)^{E} / I(q)^{1.266}}\left(f^{1.266}_{1,(Mg)(CL)} + f^{1266}_{1,(O)(CL)}\right) - f^{E}_{1,(O)(CL)} \quad (3a)$$

For Al-Mg alloy samples, neglecting the difference in atomic volume, eq.(2) gives

$$f^{E}_{1(Mg)} = f^{E}_{1(Al)(CL)} - \sqrt{I(q)^{E} / I(q)^{1.266}}\left(f^{1.266}_{1(Mg)(CL)} - f^{1.266}_{1(Al)(CL)}\right) \quad (3b)$$

where $I(q)^{E}$ is the SAXS intensity at the photon energy E, and the atomic scattering factors with (CL) are the values from Cromer-Lieberman calculations. The scattering factors evaluated by equations (3a) and (3b) are shown in Fig.3(c). They agreed well each other, although the contrast change at the absorption edge is opposite. This means that the SAXS signal from Al-Mg alloy does not contain scattering components from voids.

Present results on two-dimensional SAXS of aged Al-15.8 %Mg alloy samples showed that enhancement of weak contrast by ASAXS at the K absorption edge of Mg was successfully performed. Growth of GP zones with time and accompanying development of anisotropy were evaluated as an average over macroscopic volume. Present approach of ASAXS measurements in tender X-rays region down to 1.25 keV is useful in quantitative analysis of anisotropic nanostructure in the samples in particular characterized by large volume fraction and poorly ordered nature.

Acknowledgments

Present work has been supported by grant-in-aid for scientific research from JSPS, proposal number 25286085 and Light Metal Education Foundation. SAXS measurements have been performed under proposal 2015B1438 and 2016A1408 of SPring-8 and 2012G117,

2014G143 of Photon Factory, KEK Japan.

References

1) D.Engler, J.Hirsh, Mater. Sci. Engineering A, **336**, 249,(2002).
2) D.J.Chakrabarti, D.E. Laughlin, Prog. Mater. Sci. **,49,** 389 ,(2004).
3) S.R. Agnew and J.F. Nie, Scripta Mater. **63**,671,(2010).
4) G. Kotorz, *Physical Metallurgy*, 4th Ed. Ed. By R.W.Cahn and P.Haasen. Chapt.12 pp.1115-1199.
5) L.A.Feign and D.I. Svergun, Structure analysis by small-angle X-ray and neutron scattering, (Spinger, N.Y.1987) pp 25-28.
6) P.A. Laggner, Small-angle X-ray scatteing, ed. O.Glatter, O.Kratky (Academic Press, London 1982) chapt.10 pp.329-360
7) R.Nozato, S.Ishihara, Trans. Japan Inst. Metals, 21,580,(1980).(in Japanese)
8) T.Sato, Y.Kojima and T.Takahashi, Metall. Trans. **13A**, 1373 (1982).
9) K.Osamura, T. Ogura, Metall. Trans. **15A,** 835,(1984).
10) J.M.Raynal and M.Roth, J.Appl. Crystallgr. **8**, 535 (1975).
11) M.J.Starink and A.M. Zahra, Phil. Mag. A76 , 701-714(1997).
12) R.B.Nicholson J. de Physique et le Radium,**23**,824(1962).
13) A. Chandhuri, M.A.Singh, B.J. Diak, C. Cuoppolo, A.R.Woll, Phil Mag. **93**, 4392,(2013).
14) H.Toda, T.Hidaka,M.Kobayashi, K.Uesugi, A.Tkaeuchi, K.Horikawa, Acta Materilalia **57**, 2277, (2009).
15) N. Chouedakis, G.A.Voyoatzis J. Polym. Sci. Part B Polymer Phys. **45**, 2509,(2007).
16) H.B. Stuhrmann, J. Appl. Crystallogr. **40**, s23-s27 (2007).
17) H.Okuda, T.Yamamoto, K.Takeshita, M.Hirai, K.Senoo, H.Ogawa, Y.Kitajima, Japn. J. Appl. Phys. **53**, 05FH02,(2014).
18) J.P.Simon, O.Lyon, Acta Metall., **37**,1727, (1989) .
19) O.Lyon, J.P.Simon Phys.Rev. **B35** , 5164,(1987).
20) H.Okuda, Y.Meazawa, Y.Yokoyama, S.Kohara, S.Ochiai, Mater. Trans. **56**,774,(2015).
21) O.Lyon, *Methods in the determination of partial structures* ed. J.B.Buck et al, (World Scientific, Singapore 1993) pp.142-150.
22) J.Wernecke, C.Gollwitzer, P.Muller, M.Krumrey, J.Synchrotron Rad. **21**, 529,(2014).
23) J.Wernecke,H.Okuda, H.Ogawa, F.Siewert, M.Krumrey, Macromolecules **47**,5719, (2014).
24) T.Sato and A. Kamio, , Mater. Sci. and Eng. **A146,**161, (1991).

25) Y.Tamenori, H. Ohashi, E.Ishiguro, T.Ishikawa, Rev. Sci. Instr. **73**,1588,(2002).
26) H.Okuda, R.Sakohata, Y.Kitajima, Y.Tamenori, J. Appl. Crystallgr. **49**, 1803(2016).
27) T.C.Huang, H.Toraya, T.N.lanton, Y.Wu, J. Appl. Crystallgr., **26**,180, (1993).
28) M.J. Starink. A.M. Zahra Acta Mater. **46**,3381, (1998).
29) M.Boucher, D.Hamana, T.Laoui, Phil. Mag. A73,1733(1996).
30) H.Okuda, I.Tanaka, T.Matoba,K.Osamura, Y.Amemiya, Z. Metallkde, **88,**612 ,(1997).
31) A.Guinier, G.Fournet, Small-Angle X-ray Scattering, (John Wiley & Sons, London, 1955).
32) G.Porod, Small-angle scattering of X-rays, Ed. O.Glatter, O.Kratky, (Academic Press, N.Y.,1982). Chapt. 2, pp17-52.
33) D.T.Cromer and F.Liberman J. Chem. Phys. **53**,1891,(1970).
34) http://usaxs.xray.aps.anl.gov/staff/ilavsky/AtomicFormFactors.html

Figure Captions

Fig. 1. Differential scanning calorimetry (DSC) curve obtained for Al-15.8Mg alloys aged at 313 K. Dissolution peak of GP zones are well separated from formation and dissolution of beta' and beta phase, reported at much higher temperatures above 470 K.

Fig. 2. T wo-dimensional SAXS profile of Al-Mg samples annealed at 313 K for (a) 1 day, (b) 3 days, and (c) 2 weeks.

Fig. 3. ASAXS profiles for (a) Al-Mg alloy samples, (b) MgO, and (c) $f_{1(Mg)}$ calculated from MgO and Al-Mg ASAXS intensities.

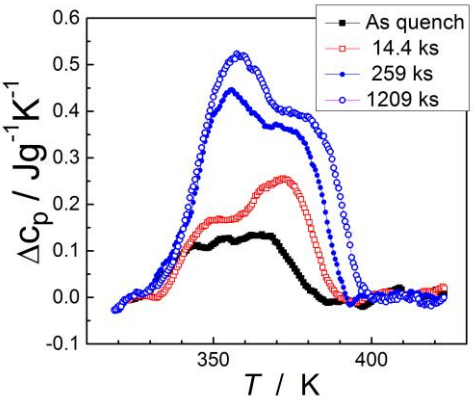

Fig.1.

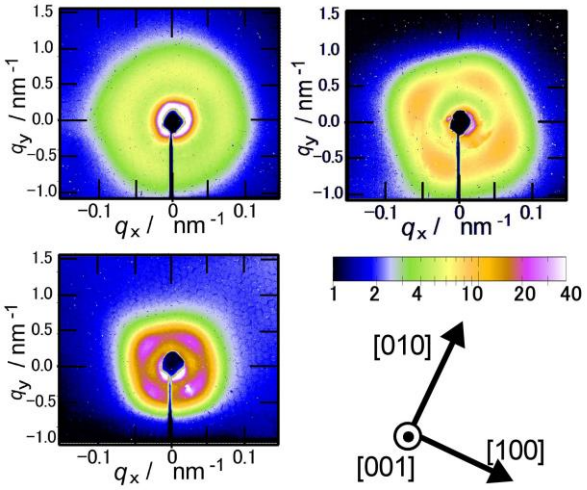

Fig. 2.

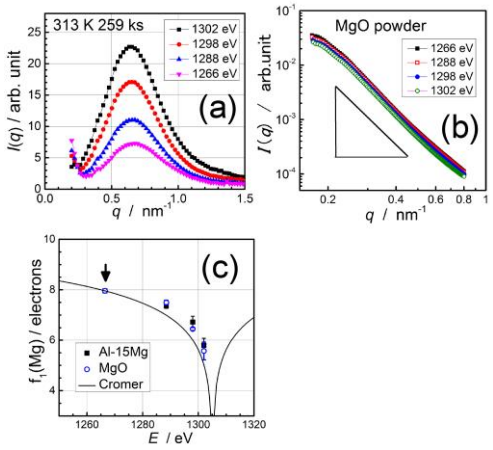

Fig. 3.

Released January 2014